EasyChair Preprint

№ 10619

Evaluating the Improvement in Shear Wave Speed Estimation Affected by Reflections in Tissue

Sy Hiep Nguyen, Quang Hai Luong, Duc Nghia Tran,
Thi Thuong Vu, Hoang Trung Nguyen and Duc Tan Tran

November 3, 2023

Evaluating the Improvement in Shear Wave Speed Estimation Affected by Reflections in Tissue

Nguyen Sy Hiep[1], Luong Quang Hai[2], Tran Duc Nghia[3], Vu Thi Thuong[4], Hoang Trung Nguyen[5], Tran Duc Tan[6*]

[1]University of information and communication technology
Thai Nguyen, Vietnam

Nshiep@ictu.edu.vn

Le Quy Don Technical University, Hanoi, Vietnam

luonghai@mta.edu.vn

[3]Institute of Information Technology, Vietnam Academy of Science and Technology, Hanoi, Vietnam

nghiatd@ioit.ac.vn

[4]Phuong Dong University, Hanoi, Vietnam

thuongvt@dhpd.edu.vn

[5]General Department of Defense Industry, Hanoi, Vietnam

trungcnqp86@gmail.com

[6]Phenikaa University, Hanoi, Vietnam

tan.tranduc@phenikaa-uni.edu.vn

Abstract. Elastography has emerged as a promising technique for non-invasive clinical diagnosis in recent years. This method estimates tissue elasticity by analyzing the speed of shear waves captured by an ultrasonic Doppler transducer, and offers several advantages such as high reliability, low cost, and non-invasiveness. However, the propagation of sliding waves in diseased tissue generates reflected waves that can affect the accuracy of the results. To overcome this limitation, this study introduces a novel technique that employs a directional filter to eliminate reflected waves and increase the reliability of the elastography results.

Keywords: Shear wave, reflection, ultrasonic, directional filter.

1 Introduction

Ultrasound elastography, which was introduced thirty years ago and has developed rapidly in recent years, is a technique for measuring the elasticity of tissue that is altered due to pathological factors. For example, a breast tumor has lower elasticity and viscosity than the healthy tissue surrounding it. Tissue elastography is applied to diagnose the liver, breast, thyroid, and prostate. Some ultrasound machines with the above features appear in machines such as the Hitachi Arietta 850, the SEQUOIA… with the specific problem mentioned in this paper. We use a vibrating needle to generate shear waves, then measure the propagation velocity in the tissue medium, thereby calculating the viscosity and elasticity of the tissue to be tested [1], [2]. the reflected wave plus the forward wave as the shear wave propagates in a heterogeneous medium in the diseased tissue. The data obtained is incorrect. To overcome this problem, We use a directional filter to remove noise [3], [4].

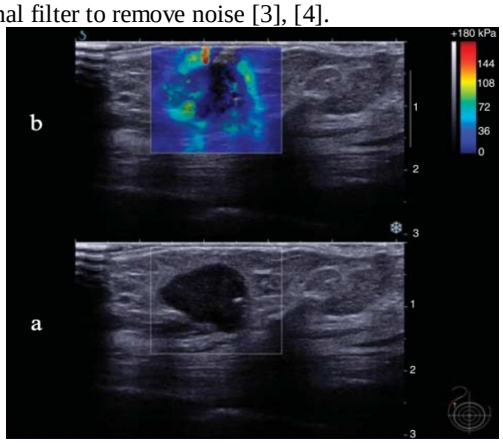

Fig. 1. (a) Greyscale ultrasound image and (b) Elastography image showing high peritumoural stiffness (mean kPa 148) [5].

1.1 Human tissue elasticity

To quantify tissue stiffness, a physical parameter known as Young's modulus is employed. This parameter is calculated by applying a uniform, external compression (or stress S) to diseased tissue, which generates a corresponding deformation (e) within the tissue. By measuring this deformation, the stiffness of the tissue can be evaluated and diagnosed.

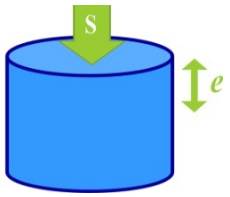

Fig. 2. Deformation of solid under an external stress.

$$E = \frac{s}{e} \qquad (1)$$

s : External stress
e : Strain in side the tissue
E :Young Modulus

Hard tissue has a higher density than soft tissue, and diseased tissue is usually harder than healthy tissue. For example, the young modulus of breast adipose tissue has a value of 18–24kPa, while the fibrous tissue has a value of 96–244kPa. Normal liver has a value of 0.4-6kPa while cirrhosis E has a value of 15-100kPa. We know the density of tissues in the body is 1000kg/m3. Normal liver has a value of 0.4-6 kPa while cirrhosis of liver E has a value of 15-100kPa. We know the density of tissues in the body is 1000kg/m3. While the density of tissue remains relatively constant in the body (1000kg/m3), tissue elasticity may differ significantly compared to tissue in a different pathological state, Compression waves propagate quickly in tissue (1500m/s), while shear waves are much slower (1–10 m/s).

The correlation between elasticity and the velocity of propagation [6].

$$E = \rho c^2 \qquad (2)$$

ρ : Density of tissues (1000kg/m^3)
c : Shear wave propagation speed
E : Elasticity

The measurement of shear wave velocity allows for the determination of tissue elasticity, given a known tissue density of 1000 kg/m^3. [6], [7], [8].

1.2 Determination of elasticity and viscosity of tissues

In this study, we used a vibrating needle to produce a shear wave that is generated by tissue expansion and propagates perpendicularly to the source in the proximal direction. The speed of shear wave propagation is determined by the stiffness of the medium, with higher stiffness resulting in greater propagation speed.

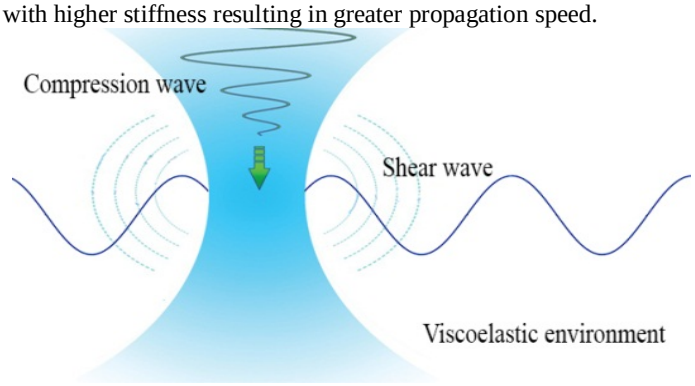

Fig. 3. The excitation source generates a shear wave.

Determine the speed of the shear wave at a position represented by the wave propagation equation. [6], [9], [10].

$$v_n(r) = \frac{1}{\sqrt{r - r_0}} A e^{-a(r-r_0)} \cos[\omega n \Delta t - k_s(r - r_0) - \phi] \tag{3}$$

Acoustic heterogeneity and tissue boundaries can cause the shear wave to undergo reflection or refraction as it propagates through tissue, which may affect the accuracy of the shear wave velocity (SWV) measurement.

Equation of the reflected wave.

$$v_n(r) = \frac{1}{\sqrt{r_0 - r}} A e^{-a(r-r_0)} \cos[\omega n \Delta t + k_s(r_0 - r) - \phi] \tag{4}$$

r	spatial coordinate	ϕ	Initial phase
r_0	coordinate of source	k_s	Wave number
A	amplitude of source	ω	Angular frequency
Δt	time step	α	the attenuation coefficient
n	the number of time step	v	velocity

According to the kelvin-voigt model, to calculate the elasticity E is also to calculate the complex shear modulus [11], [12], [13].

$$\mu = \mu_1 - i\omega\eta \tag{5}$$

For accurate location analysis, it is important to determine the elasticity and viscosity of the medium at that specific location.

Equation for viscosity and elasticity in space [6].

$$\eta = -\frac{2\rho\omega k_s \alpha}{(k_s^{\,2} + \alpha^2)^2} \tag{6}$$

μ : Complex Shear Modulus

η : Viscosity of the medium

$$\mu_1 = \frac{\rho\omega^2(k_s^{\,2} - \alpha^2)}{(k_s^{\,2} + \alpha^2)^2} \tag{7}$$

μ_1 : Tissue elasticity

ρ : Density

2 Directional filter

The reflected signal is in the opposite direction of the forward wave. The received signal is a mixed signal of the forward wave and the reflected wave. It is necessary to create a filter that removes the reflected signal. The received signal must be similar to the incoming wave signal [9].

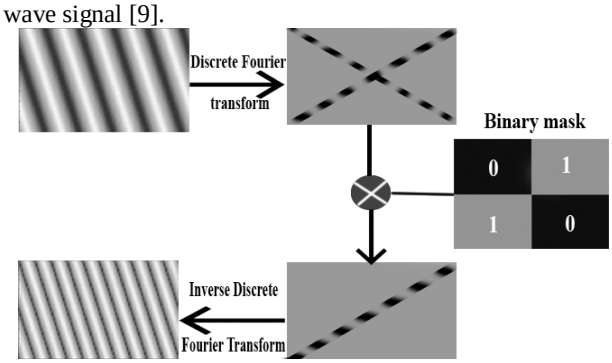

Fig. 4. Directional filter workflow.

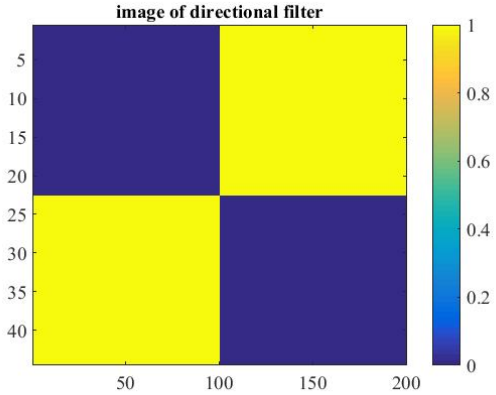

Fig. 5. Image of directional filter

The fourier-transformed input signal is then multiplied by the mask matrix Figure 5, which will determine which signals are retained and which are discarded, represented by 0 (corresponds to dark blue) and 1(corresponds to yellow). with 1 for the signal to go through and 0 to keep it. The received signal is converted back to its original form. After passing through a filter with a mask design, it moves the reflected wave from right to left. We receive the signal that is close to the incoming signal when there is no reflected noise [14].

3 System setup and results

3.1 System setup

This paper employs Matlab as a tool for simulating real-world scenarios.

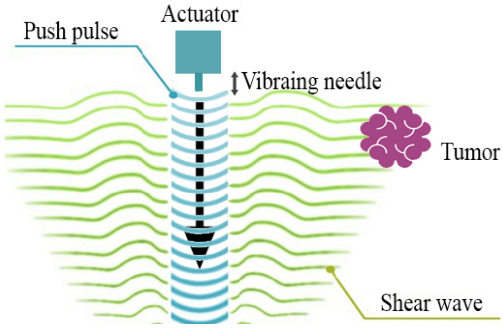

Fig. 6. Vibrating needle generate shear wave.

Details are shown in the table below.

Table 1. Parameters used for simulation.

Frequency	100Hz
Amplitude	0.0086
Normal tissue viscosity	650k Pas
Normal tissue elasticity	0.1kPa
Elasticity of diseased tissue	800kPa
Viscosity of diseased tissue	0.2Pas
Density	1000kg/m^3

Results

We evaluate the effect of the directional filter by comparing the results before and after using it.

Before using directional filter

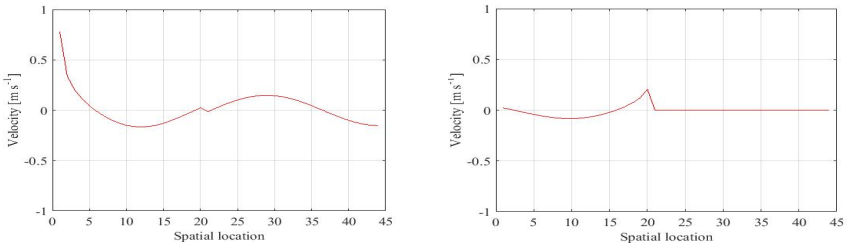

Fig. 7. (a) Incomming wave. (b) Reflected wave.

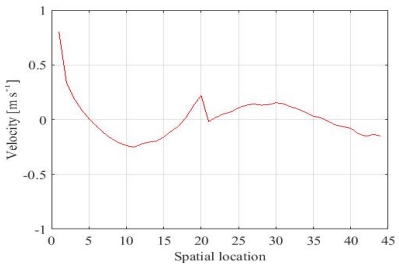

Fig. 8. Mix wave.

Observing Figure 7(b) we can see that the reflected wave starts at a location of 20 in space and then propagates from the right to the left. Figure 8 We clearly see that reflected wave affect on forward wave Figure 7(a).

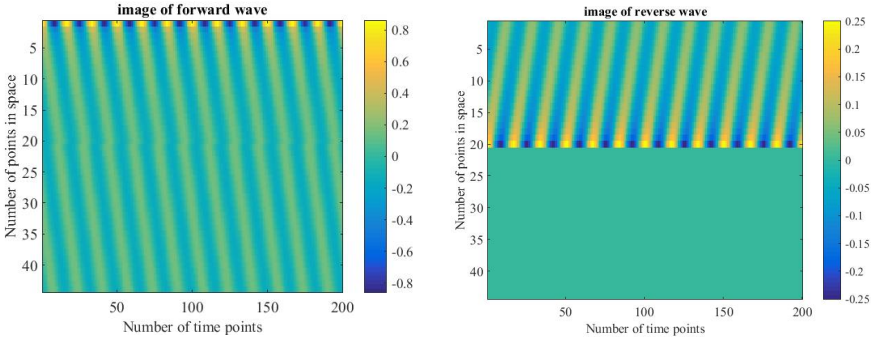

Fig. 9. (a) Image of incident wave. (b) Image of reflected wave.

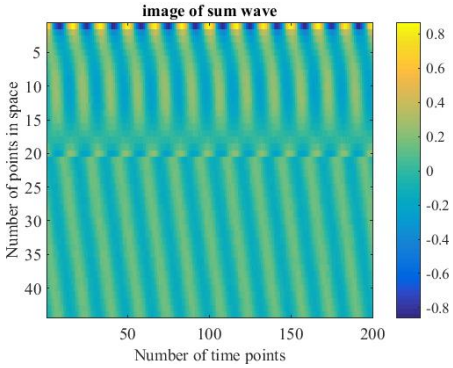

Fig. 10. Mix wave before using directional filter.

The image's color represents the wave amplitude at a specific point in time and space. For example, dark blue corresponds to wave amplitude -0.8, yellow corresponds to wave amplitude 0.8 and green corresponds to wave amplitude 0.

The creation of a mix wave image shown in Figure 10 involves the combination of the reflected wave image in Figure 9(b) and the incident wave image in Figure 9(a).

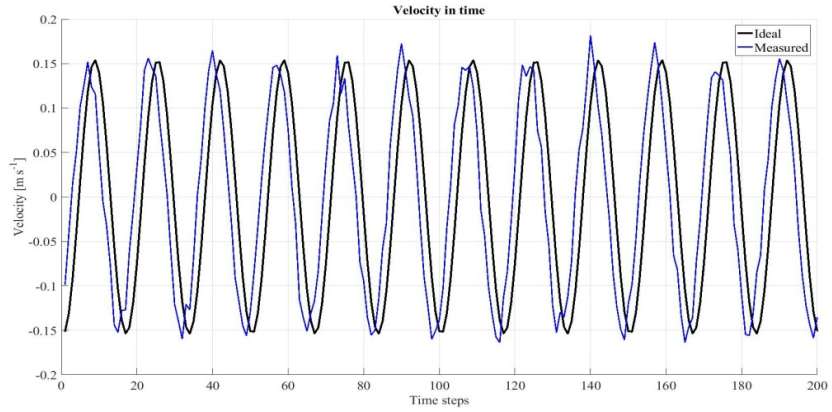

Fig. 11. The mix wave before using directional filter.

Oscillation velocity graph at position 15 in Figure 11. The received signal consists of an incoming wave signal and a reflected wave signal, so there is noise and a phase difference from the ideal waveform.

After using directional filter

Signal After being passed through the directional filter, it will remove the data oriented from right to left. Only the data of the incoming wave is kept.

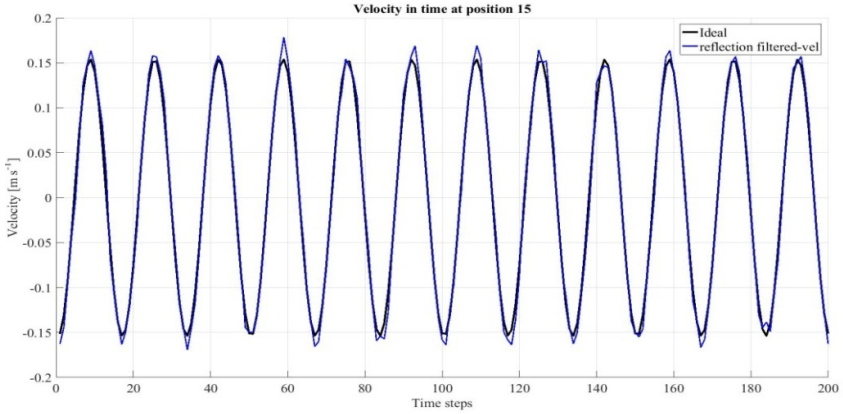

Fig. 12. The mix wave after using directional filter.

It is easy to see in Figures 11 and 12 before and after using the directional filter that the velocity graph at position 15 of Figure 12 is closer to the ideal velocity graph than in Figure 11.

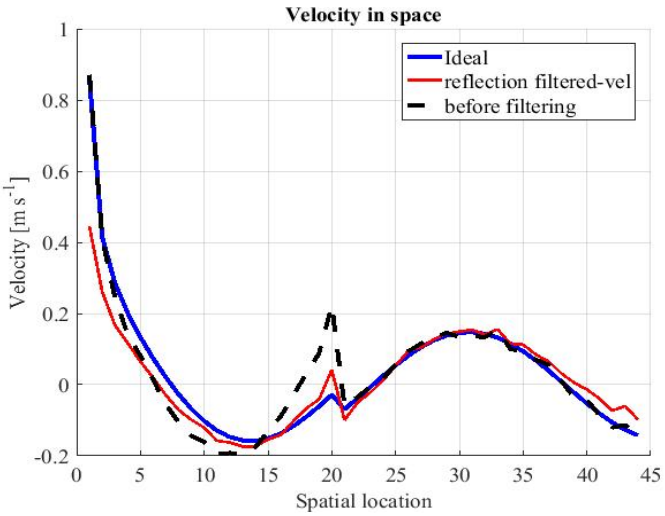

Fig. 13. Velocity in space.

In Figure 13, we observe that the blue line graph represents the ideal case, the dashed line represents the velocity graph prior to being passed through the directional filter, and the red line represents the velocity graph after it has been filtered. The red line is almost identical to the ideal velocity graph (blue line).

As depicted in Figures 7(b) and 9(b), the velocity graph begins at position 20 in space, starts at 0, ends at 45, and decreases with increasing space. The amplitude of the reflected wave is greatest at position 20, as demonstrated in the aforementioned figures, and gradually decreases until it reaches position 0. This implies that the resulting wave will be affected by the reflected wave, which is strongest at point 20 and gradually weakens as it approaches point zero, as illustrated in Figure 13. Additionally, Figures 7(b) and 9(b) indicate that the reflected wave has an amplitude of zero, as the potential does not affect the outcome of the composite wave, as shown in Figure 13.

From positions 0 to 5, the effect of the reflected wave on the composite wave is minimal, and the composite wave graph closely follows the ideal graph. Beyond position 20 (positions 25-45), the graph of the composite wave, before and after filtering, is consistent with the ideal velocity graph. In conclusion, applying directional filtering to the object from positions 5 to 25 would yield the same results as filtering from positions 0 to 45.

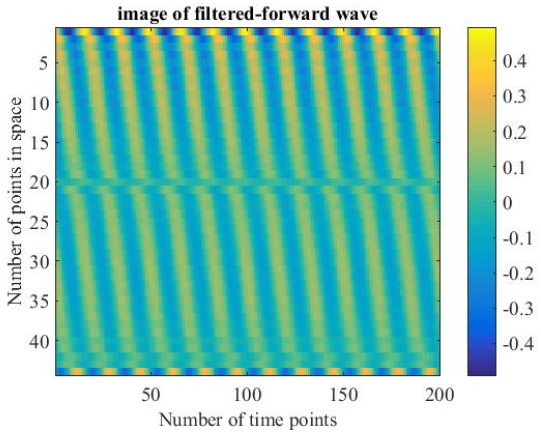

Fig. 14. Image of forward wave after using directional filter.

By using a directional filter, we can effectively eliminate and mitigate the impact of the reflected wave, resulting in an improved image of the forward wave. This improved image closely resembles the forward wave prior to filtering, leading to an increase in diagnostic accuracy.

4 Conclusion

This paper explores the effect of the reflected wave on the signal obtained in elastography. We propose the use of a directional filter to reduce its impact. Our results, obtained through simulation in Matlab, show that the filter is effective in minimizing the reflected wave. In future work, we aim to improve the filter to accommodate multi-directional signals, thereby enhancing signal quality.

References

[1] Bercoff J, Tanter M, Fink M. Supersonic, "Shear imaging: a new technique for soft tissue elasticity mapping." IEEE Transactions on Ultrasonics, Ferroelectrics, and Frequency Control, 2014.

[2] Sigrist RMS, Liau J, Kaffas AE, Chammas MC, Willmann JK, "Ultrasound elastography: review of techniques and clinical applications," Theranostics 2017.

[3] Pengfei Song1,2, Armando Manduca1, Heng Zhao1, Matthew W. Urban1, James F.Greenleaf, Shigao Chen, "Fast Shear Compounding Using Robust Two-dimensional Shear Wave Speed Calculation and Multi-directional Filtering." Ultrasound Med Biol. 2014 June, 2014.

[4] Thomas defeux, Jean-luc Gennisson, Jeremy bercoff, and Mickael Tanter "On the Effects of Reflected Waves in Transient Shear Wave Elastography." IEEE TransacTIons on UlTrasonIcs, FErroElEcTrIcs, and FrEqUEncy conTrol, vol.

58, no. 10 , 2011.

[5] Andrew Evans, Patsy Whelehan, Kim Thomson, Katrin Brauer, L Jordan, Colin Purdie, D McLean, Lee Baker, Sarah Vinnicombe, Alastair M Thompson,"Differentiating benign from malignant solid breast masses: Value of shear wave elastography according to lesion stiffness combined with greyscale ultrasound according to BI-RADS classification" British Journal of Cancer · June 2012, June 2012.

[6] Quang-Hai Luong, Manh-Cuong Nguyen, Tan Tran-Duc, "Complex shear modulus estimation using extended kalman filter." Tạp chí khoa học& kỹ thuật số179, 2016.

[7] Carlson, L.C.; Feltovich, H.; Palmeri, M.L.; Dahl, J.J.; Munoz del Rio, A.; Hall, T.J. "Estimation of shear wave speed in the human uterine cervix." Ultrasound Obstet. Gynecol. 2014, 43, 452–458, 2014.

[8] Dalong Liu Emad S. Ebbini Viscoelastic Property Measurement in Thin Tissue Constructs Using Ultrasound IEEE Transactions on Ultrasonics, Ferroelectrics, and Frequency Control. 2008 February, 2008.

[9] Nguyen Thi Hao, Tran Thuy-Nga, Vu Dinh-Long, Tran Duc-Tan, Nguyen Linh-Trung, "2D Shear Wave Imaging Using Maximum Likelihood Ensemble Filter." International Conference on Green and Human Information Technology (ICGHIT 2013), 2013.

[10] Walker WF, Fernandez FJ, Negron LA, "A method for imaging viscoelastic parameters with acoustic radiation force Phys." Med. Biol 2000;vol. 45:1437–1447, 2000.

[11] H. Yuan, B.B. Guzina, S. Chen, R.R. Kinnickb and M. Fatemi "Estimation of the complex shear modulus in tissue-mimicking materials from optical vibrometry measurements." Inverse Problems in Science and Engineering Vol. 00, No. 00, March 2011.

[12] Antonio Callejas, Antonio Gomez, Inas H. Faris, Juan Melchor and Guillermo Rus," Kelvin–Voigt Parameters Reconstruction of Cervical Tissue-Mimicking Phantoms Using Torsional Wave Elastography." Sensors 2019, 19, 3281; doi:10.3390/s19153281, 2019.

[13] Tran Quang Huy, Pham Thi Thu Ha, Tran Binh Duong,Nguyen Quang Vinh, Nguyen Thi Hoang Yen, Tran Duc Tan, "2D Shear Wave Imaging in Gaussian Noiseand Reflection Media." VNU Journal of Science: Mathematics – Physics, Vol. 37, No. 4, 2021.

[14] Shaozhen song, Nhan Minh Le, Zhihong huang "Quantitative shear-wave optical coherence elastography with a programmable phased array ultrasound as the wave source." Article in Optics Letters · October 2015 2015.